INTENSE STOPPING MUON BEAMS*

C. Y. Yoshikawa†, R. Abrams, C. Ankenbrandt, M. A. C. Cummings, R. P. Johnson
Muons, Inc., Batavia IL, USA
M. Martens, D. Neuffer, M. Popovic, E. Prebys, K. Yonehara, Fermilab, Batavia, IL, USA

Abstract

The study of rare processes using a beam of muons that stop in a target provides access to new physics at and beyond the reach of energy frontier colliders. The flux of stopping muons is limited by the pion production process and by stochastic processes in the material used to slow down the decay muons. Innovative muon beam collection and cooling techniques are applied to the design of stopping muon beams in order to provide better beams for such experiments. Such intense stopping beams will also support the development of applications such as muon spin resonance and muon-catalyzed fusion.

INTRODUCTION

Current designs of proposed muon-to-electron conversion experiments [1,2] use a solenoid around a target to collect low-momentum pions (below about 100 MeV/c) produced at large angles. The pion production cross section is small in that kinematical region. Many of the resulting decay muons spiral down a transport solenoid, and the ones that are slow enough stop in a second target. The alternative pursued here is to capture pions that are produced in the forward direction with momenta near the peak of their production spectrum. The pion capture section, a so-called Dipole and Wedge configuration, uses a 180-degree bend to create a momentum-dispersed horizontal focus. A wedge at that location renders the output pion beam nearly mono-energetic. The resulting decay muons will be cooled and degraded utilizing a new invention, the Helical Cooling Channel (HCC) [3]. The fact that the proton beam points away from the experiment, as in the original designs [1,2], helps to reduce backgrounds; this design also naturally eliminates wrong-sign particles. This configuration significantly reduces the spread of muon flight times compared to the baseline Mu2e design, providing a wider time interval for accepting candidate events and allowing the use of higher-Z stopping targets with shorter muon capture lifetimes. The HCC is momentum-dependent; that is, the magnetic field strength is reduced to match the momentum of the muons as they traverse the degrader. A previous study utilized a HCC filled with gaseous hydrogen of variable density [4], while a more recent version used LiH wedges with variable spacing [5]; both showed promising results. This paper optimizes the Dipole and Wedge apparatus, weighing cost and performance. Preliminary results of matching between the Dipole and Wedge and the HCC are also presented.

*Supported in part by DOE STTR Grant DE-FG02-07ER84824 and FRA DOE Contract DE-AC02-07CH11359
†cary.yoshikawa@muonsinc.com

DIPOLE AND WEDGE CAPTURE

The general layout of the Dipole and Wedge, the momentum-dependent HCC, and the matching section are shown in Figure 1. The production of π^- and μ^- from 8 GeV protons on a gold target was simulated in MARS [6]. G4beamline [7] is then used to study various configurations of the Dipole and Wedge capture system.

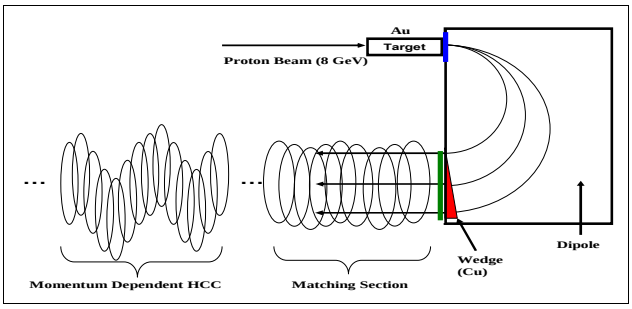

Figure 1: Layout of Dipole and Wedge (Cu), momentum dependent HCC, and the matching section. The blue line indicates where π^- and μ^- from the target are generated to study various Dipole/Wedge configurations. The green line shows the location of a circular aperture immediately behind the wedge.

Figure 2 shows the momentum spectrum of π^- and μ^- produced off the target. The momentum acceptance of various configurations is also indicated. For consistency with a set of real test HCC coils that were constructed at Fermilab [8], all configurations had a circular aperture with 25 cm radius at the wedge exit.

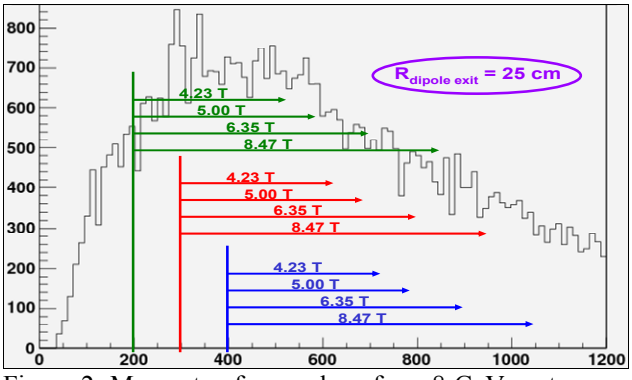

Figure 2: Momenta of π− and μ− from 8 GeV protons on a gold target, 16 cm in length and 6 mm in diameter, simulated in MARS. Table 1 below contains details of the configurations highlighted here. For example, the second entry in Table 1 has the lowest momentum accepted, P_{low} = 200 MeV/c, and B_{dipole} = 5 T.

Figure 3 shows the corresponding apparatus and its resulting performance. Figure 3 (a) is a top view of the trajectories of pions and muons resulting from 8 GeV protons hitting a gold target (length = 16 cm, diameter = 6 mm as in Mu2E). The (red) negatively charged particles (mostly π^-) bend in a dipole field with B = 5 T. Those in the design momentum range traverse the Cu wedge. Negative pions with momentum of 200 MeV/c (P_{low}) strike the thin edge of the wedge closest to the production target. The aperture at the dipole exit (0.5 m diameter) along with B_{dipole} = 5 T constrain P_{high} to be 575 MeV/c. (This momentum range, 200 to 575 MeV/c, is also shown in Figure 2.) The amount of Cu wedge material to degrade π^-'s with P_{high} = 575 MeV/c down to P_{low} = 200 MeV/c defines the length of the thick side of the wedge, which corresponds to 1.8 λ_I of Cu. Figure 3(b) shows the momentum/position correlation to be exploited by using the wedge degrader. There are a few pions with momentum higher than the ideal. As shown in Fig. 3(f), these higher-momentum pions at a given exit location emerge from the target with large production angles; the focusing works well for angles up to about 300 mrad. The momentum/position correlation plot of Figure 3(c) shows a mono-energetic beam of pions emerging from the wedge. Figure 3(e) is the momentum projection of (c) (note reversal of direction in histogram). For 100k protons on target (POT), 3914 π^- and μ^- are headed toward the momentum-dependent HCC. However, we impose a cut of 276 mrad on the polar angle to match the expected acceptance of the downstream momentum-dependent HCC, resulting 1061 π^- and μ^- after the wedge that are forward-going and destined for the momentum dependent HCC, as tallied in Table 1.

Table 1 gives the expected yield for each configuration simulated, and Figure 2 shows the range of momenta accepted by those configurations with respect to the production spectrum. Figure 4 shows the expected yield to elucidate the tradeoffs between performance and cost.

Table 1: Results for various Dipole/Wedge configurations

P_{low} (MeV/c)	P_{high} (MeV/c)	B_{dipole} (T)	$\#\lambda_{I,Cu}$ ($\lambda_{I,u}$=15.32 cm)	N($\pi-\&\mu-$) per 100k POT R ≤ 25 cm θ ≤ 276 mrad
200	517	4.23	1.5	912
200	575	5.00	1.8	1061
200	676	6.35	2.3	1263
200	835	8.47	3.0	1337
300	617	4.23	1.5	885
300	675	5.00	1.8	1135
300	776	6.35	2.3	1367
300	935	8.47	3.0	1401
400	717	4.23	1.5	807
400	775	5.00	1.8	1015
400	876	6.35	2.3	1272
400	1035	8.47	3.0	1428

Figure 4 shows the pion yield rising until about B_{dipole} = 6.35 T, with P_{min} = 300 MeV/c being best. However, we choose B_{dipole} = 5 T as a practical limit above which the magnet technology becomes more difficult. With that restriction, P_{min} = 300 MeV/c provides only marginal improvement over P_{min} = 200 MeV/c. Experience with simulations of cooling in this low momenta regime favors the choice of P_{min} = 200 MeV/c.

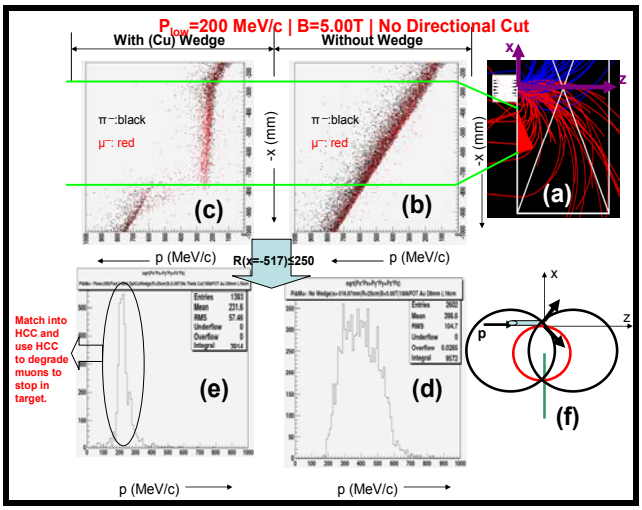

Figure 3: The Dipole/Wedge configuration with P_{low} = 200 MeV/c and B_{dipole} = 5 T. (a) Top view of pions and muons in Dipole/Wedge. Negatively (positively) charged particles are red (blue). (b) Correlation between momenta and horizontal exit position from dipole for π^- and μ^- without a wedge. (c) Correlation between momenta and horizontal exit position from dipole for π^- and μ^- with wedge. (d) Momentum projection from "b." Note direction reversal of p for "d" and "e." (e) Momentum projection from "c." (f) Cartoon explaining momentum asymmetry in "b"; see text.

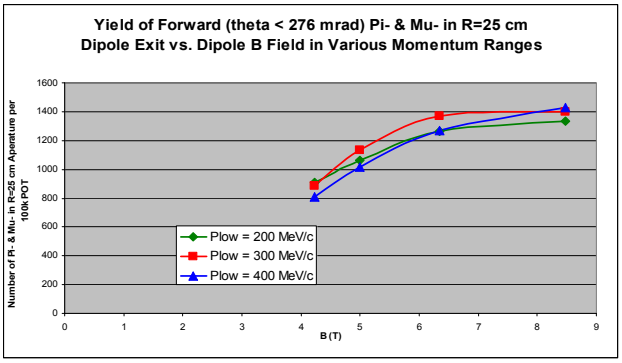

Figure 4: Yields for various configurations of Dipole and Wedge apparatus. Data are from Table 1.

MOMENTUM DEPENDENT HCC

The Pmin = 200 MeV/c / Bdipole = 5 T configuration for pion capture has its peak momentum flux at 220 MeV/c. For that momentum, the average momentum of the decay muons is 175 MeV/c. Hence, the momentum-dependent HCC is designed to stop muons that enter it with 175 MeV/c. We followed the same prescription [5] in constructing a momentum dependent HCC by positioning 1 mm thick LiH slabs with variable spacing to

match the linear reduction in momentum of the reference muon and the associated HCC solenoid, dipole, and quadrupole fields. The HCC has a reference orbit radius of 25 cm, pitch angle of 45 degrees, and 4 complete helical periods for a total length of 6.28 m. Figure 5 shows the momentum distribution of muons near the end of the momentum dependent HCC, where the initial muon beam consists of 1000 ideal muons at 175 MeV/c injected on the reference trajectory. Muons with momenta below 50 MeV/c will stop almost all the time in the default Mu2e stopping target, with diminished stopping probability up to 75 MeV/c [1] depending on the entrance angle.

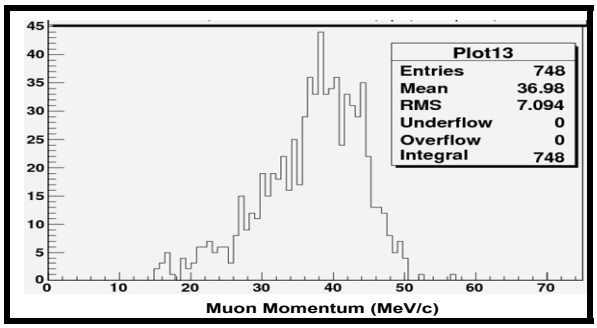

Figure 5: Momentum of muons at end of momentum-dependent HCC after 1000 muons with 175 MeV/c were injected at the start on the reference orbit.

MATCHING FROM DIPOLE/WEDGE INTO MOMENTUM-DEPENDENT HCC

To match between the downstream HCC and the upstream Dipole/Wedge, we followed an empirical solution that was found to work well for another proposed experiment, the MANX experiment [9]. Coils and currents are constrained to match at the entry into the HCC. The aperture, current, and helix period were kept constant in the match going upstream to the Dipole/Wedge, but the radius of the helix (and hence the pitch, since the period is constant) was linearly reduced to zero at the start of the matching section (the exit of the Dipole/Wedge).

Initial simulations of the system for 8 GeV protons on the gold target yielded a low rate of slow muons ($p \leq 50$ MeV/c) at the end of the HCC. We attribute this low rate to mismatching between the end of the Dipole/Wedge and the start of the matching section. Figure 6(a) shows the momentum distribution at the start of the matching section for pions produced from 8 GeV protons on the gold target that are forward-going after the wedge. Figure 6(b) shows the "momentum acceptance" of the matching section that maps parent pions at the start of the matching section to daughter muons that fall into the kinematic region to be stopped ($p \leq 50$ MeV/c). There is a mismatch which must be addressed in future iterations in designing the matching section and its downstream HCC. Some focusing between the wedge and the entrance to the matching section is probably needed.

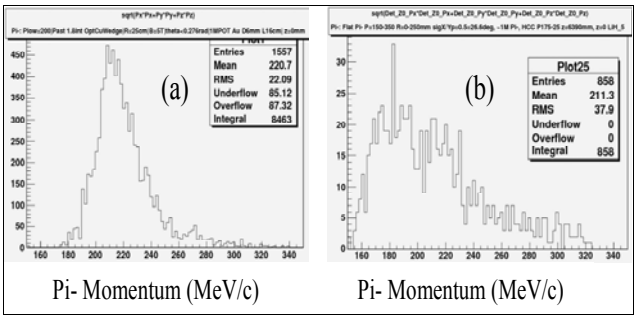

Figure 6: Mismatch of pion momenta at entrance to the matching section. (a) Momentum distribution of forward going pions ($\theta \leq 276$ mrad) from a million protons on a gold target, passing wedge and entering matching section. (b) Pion momentum distribution of parent pions with daughter muons that would be stopped near end of momentum dependent HCC.

SUMMARY AND OUTLOOK

A system to capture, cool, and stop muons in a target using a Dipole/Wedge capture system and a momentum-dependent HCC, with a matching section between them, was designed. The Dipole/Wedge was optimized by considering yield vs. cost. The matching section transfers pions from the upstream Dipole/Wedge to muons in the downstream HCC. Mismatches were uncovered, and future work will focus on their remedy.

REFERENCES

[1] Mu2e Experiment: http://mu2e.fnal.gov/

[2] COMET Experiment: Y. Kuno et. al, "An Experimental Search for Lepton Flavor Violation $\mu^- - e^-$ Conversion at Sensitivity of 10^{-16} with a Slow-Extracted Bunched Proton Beam", An Experimental Proposal on Nuclear and Particle Physics Experiments at the J-PARC 50 GeV Proton Synchrotron, November 30, 2007.

[3] Y. Derbenev and R. P. Johnson, Phys. Rev. STAB 8, 041002 (2005)

[4] M. A. C. Cummings, R. P. Johnson, Charles Ankenbrandt, Katsuya Yonehara, THPMN096, PAC07

[5] M. A. C. Cummings, R. Abams, R. P. Johnson, C. Y. Yoshikawa, C. Ankenbrandt, M. Martens, D. Neuffer, K. Yonehara, MOPP071, EPAC08

[6] MARS, http://www-ap.fnal.gov/MARS/

[7] G4beamline, http://g4beamline.muonsinc.com

[8] V. S. Kashikhin, N. Andreev, A. N. Didenko, V. Kashikhin, M. J. Lamm, A. V. Makarov, K. Yonehara, A. V. Zlobin, R. P. Johnson, S. A. Kahn, "4 Coil HCC", WEPD013, EPAC08

[9] MANX: R. Abrams, M. A. Cummings, S. Kahn, C. Ankenbrandt, R. P. Johnson, M. Lamm, A. Zlobin, V. Kashikhin, K. Yonehara, WEPP153, EPAC08